Vol. 45, No. 2 (2023) 191-200, DOI: 10.24874/ti.1372.09.22.03

Tribology in Industry

www.tribology.rs

RESEARCH

# Tribo-layer Properties on AISI52100 Lubricated by Palm Methyl Ester Containing Graphene Nanosheet

Zahrul Fuadi[a,*], Rudi Kurniawan[a], Farid Mulana[b]

[a]*Mechanical and Industrial Engineering Department, Universitas Syiah Kuala, Banda Aceh, Indonesia,*
[b]*Chemical Engineering Department, Universitas Syiah Kuala, Banda Aceh, Indonesia.*

Keywords:

*Friction*
*Wear*
*Tribofilm*
*Eco-friendly lubricant*
*Renewable lubricant*

* Corresponding author:

*Zahrul Fuadi*
*E-mail: zahrul.fuadi@usk.ac.id*

*Received: 19 September 2022*
*Revised: 31 October 2022*
*Accepted: 17 March 2023*

A B S T R A C T

*The demand for bio-degradable lubricants has been increasing nowadays due to concerns on pollution free environment. Vegetable oil-based lubricant is one of promising sources of lubricant that can fulfill the requirement, especially when combined with eco-friendly nanomaterial additives. On the other hand, tribo-layer formation as the mechanism of friction and wear reduction in a tribo-pair has been generally accepted in tribology field. The tribo-layer layer can be formed due to the tribo-chemical reaction during friction process and its formation can be enhanced with incorporation of nanomaterials as additive. In this study, the tribo-layer characteristics formed on self-mated AISI52100 contact pair were investigated. The contact pair were lubricated by two kind of lubricant's specimens, i.e. palm methyl ester (PME) and palm methyl ester containing graphene nanosheet additive. It is found that in the case of palm methyl ester without graphene additive, the tribo-layer comprises oxidative layer of Fe and O elements. With the presence of graphene nanosheets in the lubricant, the tribo-layer was formed in a comparatively wider contact area. Carbon element was more observable in the layer besides oxygen, emphasizing the role of graphene nanoparticles. In both cases, the friction coefficient and wear are relatively similar.*



## 1. INTRODUCTION

Efficient operation of components in a mechanical system requires effective lubrication of the interacting parts to protect them from excessive friction and wear. Mineral oil has been used as lubricant based material and with the use of additives, thanks to the developments in material technology that provides various functional materials in nanometer dimension as additives, its performance has been significantly improved. However, mineral oil-based lubricants, beside its reserve's exhaustion issue, possess significant environment threats due to disposal contamination problems. It has toxicity problem and not readily bio-degradable [1,2], contaminating the soil, air, water source and ecological life in a wide extent. Therefore, the demand for eco-friendly lubricants is increasing, together with people's expectation for pollution-free environment.

Vegetable oils have been treated as the main option to achieve this requirement of environment friendly lubricants. Among the sources are coconut, sesame, soybean, corn, rapeseed, jojoba, olive, jatropha, castor oil, palm, cotton seed, sunflower, etc. Many of them are found to have great potential to be used as lubricant due to their desirable property of good lubricity [3], besides renewability and bio-degradability ready. One of the most widely used vegetable oils in automotive and industry nowadays is palm oil [4]. This is because it can be readily used as a substitute for diesel engine fuel and therefore also potential as a lubricant base material. The total production of crude palm oil was 63.4 million tons in 2020 [5] and a significant percentage of it was processed for biodiesel fuel.

Researches about tribological properties of palm oil have been conducted by many researchers. Palm oil, in esterified form of palm methyl ester, is found beneficial when used as either a mixture in mineral diesel fuel or additive in mineral oil lubricant. Pure palm methyl ester, when used as lubricant to cast iron tribo-pair, produced lower wear than mineral diesel fuel [6]. When used as additive in mineral oil lubricant, it also reduced the friction and wear of the tribo-pair compared to the lubricant in its original state [7]. Lower friction and wear can be achieved due to the formation of protective film on the contact interface by tribo-chemical reaction [8,9].

Nanomaterials, on the other hand, have also been incorporated into oil-based lubricants to achieve desirable tribological properties of the lubricants. Nanomaterials as additives can be classified into three groups, i.e. nanometal-based, nanocarbon-based, and nanocomposite-based [10]. One of emerging nanomaterials, graphene, has been found to be highly effective as a lubricant additive due to its high specific surface area, weak interlayer interaction, good chemical stability, and eco-friendly nature. Tiny amount of graphene additive in a lubricant could reduce the friction on a tribo-pair. This can be achieved due to the nanoparticle's capability to produce nano-scrolls [11] or nano-bearing layer acting as protective film [12,13] at the sliding surfaces. In addition, graphene nanoparticle also has a capability to create transformation at the microscale level that promotes interlayer sliding, and such a synergetic effect resulted in significant reduction of friction and wear [14,15,16].

The incorporation of nanoparticles as lubricant additive in palm oil has also been the subject of investigations. The tribological properties of palm oil are found improved by incorporation of Boron Nitride nanoparticles [17], while CuO and MoS2 nanoparticle additive also increased the anti-wear property of chemically modified palm oil in extreme pressure condition [18]. Carbon coated aluminum nanoparticles [19] and nano-graphene oxide particles [20] were also found beneficial as additive in palm oil diesel fuel due to their capability to improve the diesel engine's emission performance.

Despite various reports on the application of nanoparticle as additives in palm oil, the tribological properties of palm methyl ester with graphene nanoparticles as additives has not much been discussed, particularly from the point of view of tribo-layer formation. In this study, graphene particles in nanosheet form was added to palm methyl ester to study the tribological behaviour of a tribo-pair lubricated by the modified fluid. The investigation focuses on the tribo-layer characteristic formed on the sliding interface of self-mated bearing steel (AISI52100). The result is compared to that in the case of palm methyl ester without the graphene nanoparticles.

## 2. LUBRICANT PREPARATION AND EXPERIMENTAL SETUP

This study consists of several steps, i.e. preparation of the lubricant and friction material, friction test, and wear evaluation. Each step is explained as follows:

### 2.1 Lubricant preparation

Two lubricant samples (S1 and S2) were prepared for this study (Fig. 1). The sample S1 is palm methyl ester (PME). The methyl ester has a viscosity of 4.415 $mm^2/s$ at $40^oC$. Its main components are methyl palmitate, oleic acid, and methyl stearate [8]. A small amount of glycerol can be expected as the side products of transesterification process. The palm methyl ester was obtained commercially.

Lubricant sample S2 (Fig. 1) was prepared by mixing 1 mg of graphene particles into 50 ml of PME. The graphene particles used, shown in

Fig. 2, is in sheet form with approximate thickness of 0.1 μm. To achieve a good mixture between the graphene and PME, the solution was put in the ultrasonic bath for an hour.

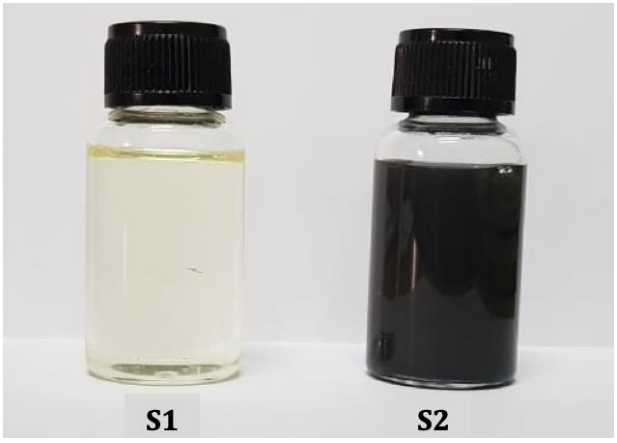


**Fig. 1.** Lubricant specimens: S1 (palm methyl ester), S2 (palm methyl ester + graphene).

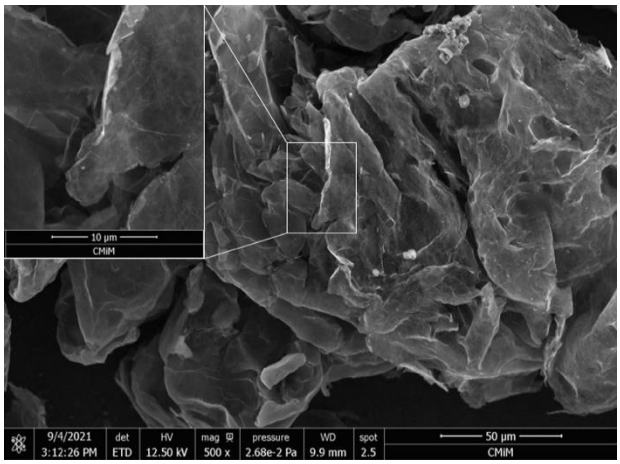


**Fig. 2.** Graphene nanosheets.

The stability of the mixture (lubricant sample S2) is evaluated using sedimentation method, i.e. by evaluating the image captured after certain sedimentation periods (Fig. 3). This method of evaluation is simple yet effective and has been applied elsewhere, for example in [21,22]. Fig. 3 shows that sedimentation of graphene particles has already been visible at one day after the mixture preparation. Most of the graphene particles have already sedimented after 8 days. Apparently, this is caused by the lumped condition of the graphene sheets. As seen in Fig. 2, despite extremely thin, the graphene sheet is in folded form that can have a size of several hundreds micrometers. The size of graphene flakes is not uniform and it does not have the ability to maintain its planar shape after dispersion into lubricants [23].

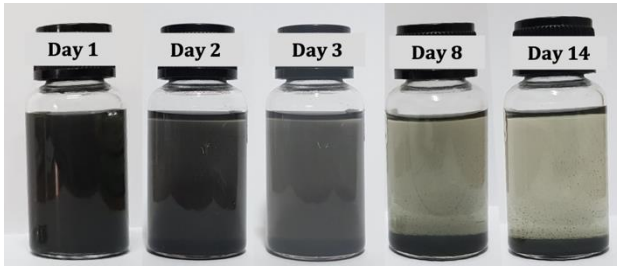


**Fig. 3.** Stability of the lubricant sampleS2.

## 2.2 Friction test

The friction tests were conducted using a reciprocating pin-on-disk tribometer (Fig. 4a). The tribometer consists of a cantilever beam used as the force sensor and the disk holder installed on a reciprocal moving table. The cantilever beam is supported by a shaft installed on two radial bearings so that the normal load can be applied using gravitational weight. A pin is installed on the cantilever beam and put in contact with the disk moving in back and forth direction. A small amount of lubricant can be supplied to the contact interface.

The material of both pin and disk are SUJ2 (AISI52100, E = 210 GPa, Poisson's ratio = 0.3), commonly used for bearing material. The pin is 5 mm in diameter and has a hemispherical contact surface with a contact radius of 10 mm. The disk is 40 mm in diameter and 5 mm thick. The surface of contact areas of both the pin and the disk were polished using emery paper up to grid #10000.

One of the most important characteristics of a lubricant is its ability to protect the contact interface during a severe contact condition. Such condition occurs either at an extremely high contact pressure or a low sliding speed where significant amount of material direct contact on the contact interface takes place. In such condition, the lubrication's performance is decided by the ability of the fluid to form a protective layer on the contact interface to protect the material from excessive friction and wear. To simulate such severe contact condition, in this study, the friction tests were conducted at a normal force of 10 N, resulting in the initial Hertzian contact pressure of 1.2 GPa to the contact pair. The friction tests were conducted at temperature of 65±2°C.

In the friction test, the disk moves in reciprocating direction. The sliding distance of one complete cycle is 15 mm, completed in 3 s. The sliding velocity is 0.2 m/s except at the edges of the sliding

track, which is 0 m/s. A friction test was conducted for a total of 4 hours with a sampling frequency of 10 Hz; 4800 cycle or 72 m sliding distance. The friction force was acquired using two strain gauges installed on the beam. KYOWA EDX-10B/15-A system was used to record the friction data.

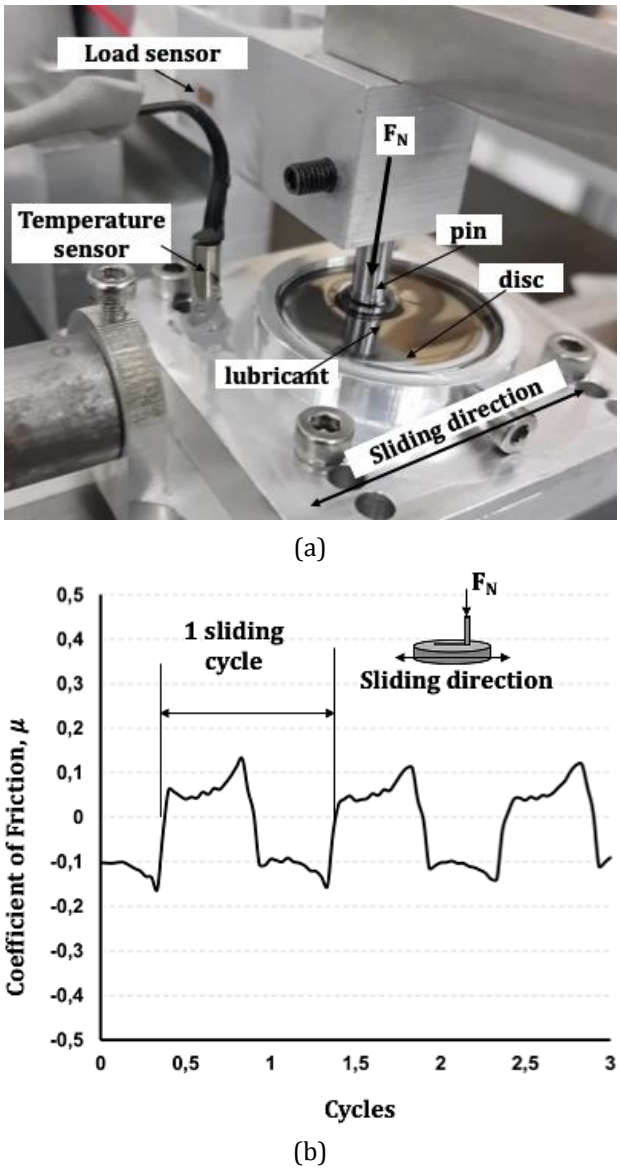


**Fig. 4.** Reciprocating pin-on-disk tribometer (a), friction coefficient acquired from one-sliding-cycle: negative value of friction indicates sliding in reverse direction (b).

Fig. 4b illustrates the recorded friction data from a few sliding cycles. A U-shape curve can be observed in each half-cycle friction curve, indicating the static friction coefficient at the point where sliding velocity reaches zero. A complete cycle consists of both positive and negative Coefficient of Friction (CoF) value. Negative value of friction coefficient indicates the sliding in the reverse direction.

### 2.3 Wear analysis

Since the pin was in constant contact during the sliding, the wear analysis focused on the worn area of the pin. The analysis was conducted with Scanning Electron Microscope together with Energy-dispersive X-ray Spectroscopy.

## 3. RESULTS AND DISCUSSION

Fig. 5 shows the friction coefficient of both S1 and S2 condition for the entire 4800 test cycles; 72 meter sliding distance. In general, the friction curves show a relatively similar behaviour, i.e. started from a value of about 0.1 and gradually increased to an average of 0.2 at sliding cycle around 1000. The friction coefficient curves indicate a similar value from sliding cycle around 1400. The comparison between the friction coefficient curves of condition S1 and S2 at different sliding cycles can be observed in more detail in Fig. 5(b) to Fig. 5(e), respectively. Obviously, some differences in the friction coefficient curves of the two condition can be observed at the beginning of sliding and at sliding cycle between 1000 to 1500, as shown in Fig. 5(b) and Fig. 5(c)-(d).

Fig. 6(a) shows the result of friction tests comparing the coefficient of friction (CoF) for both lubricants S1 (PME) and S2 (PME+Graphene) for the first 3 sliding cycles shown in Fig. 5(c). One sliding cycle consists of CoF value in both positive and negative. Fig. 6(b) indicates the CoF value for the 1st half cycle. It can be observed that both CoF curves show the values increasing towards the right side; in the case of S1 the value increases from 0.06 to 0.12. This indicates that during the friction test, the disk tilted to the right side.

Fig. 6(b) shows that the inclusion of graphene particles in the methyl ester reduced the CoF significantly, an average of 40%, starting the 1st sliding cycle. This CoF reduction clearly indicates the role of graphene nanosheet in reducing the interfacial shear strength on the contact interface. Being two-dimensional in the structure and having a good chemical stability, graphene is known as having high specific surface area and weak interlayer interaction. Therefore, the graphene sheets of sub-micrometre thick could easily slide into the asperities in contact to reduce the interlayer contact resistance. It has been

reported that the super lubricity at the tribo-pair produced by graphene is attributed to the formation of nano-scrolls at the sliding interface [11]. Graphene in tiny amount as additive can also produce a nano-bearing layer to reduce the friction at the tribo-pair [12].

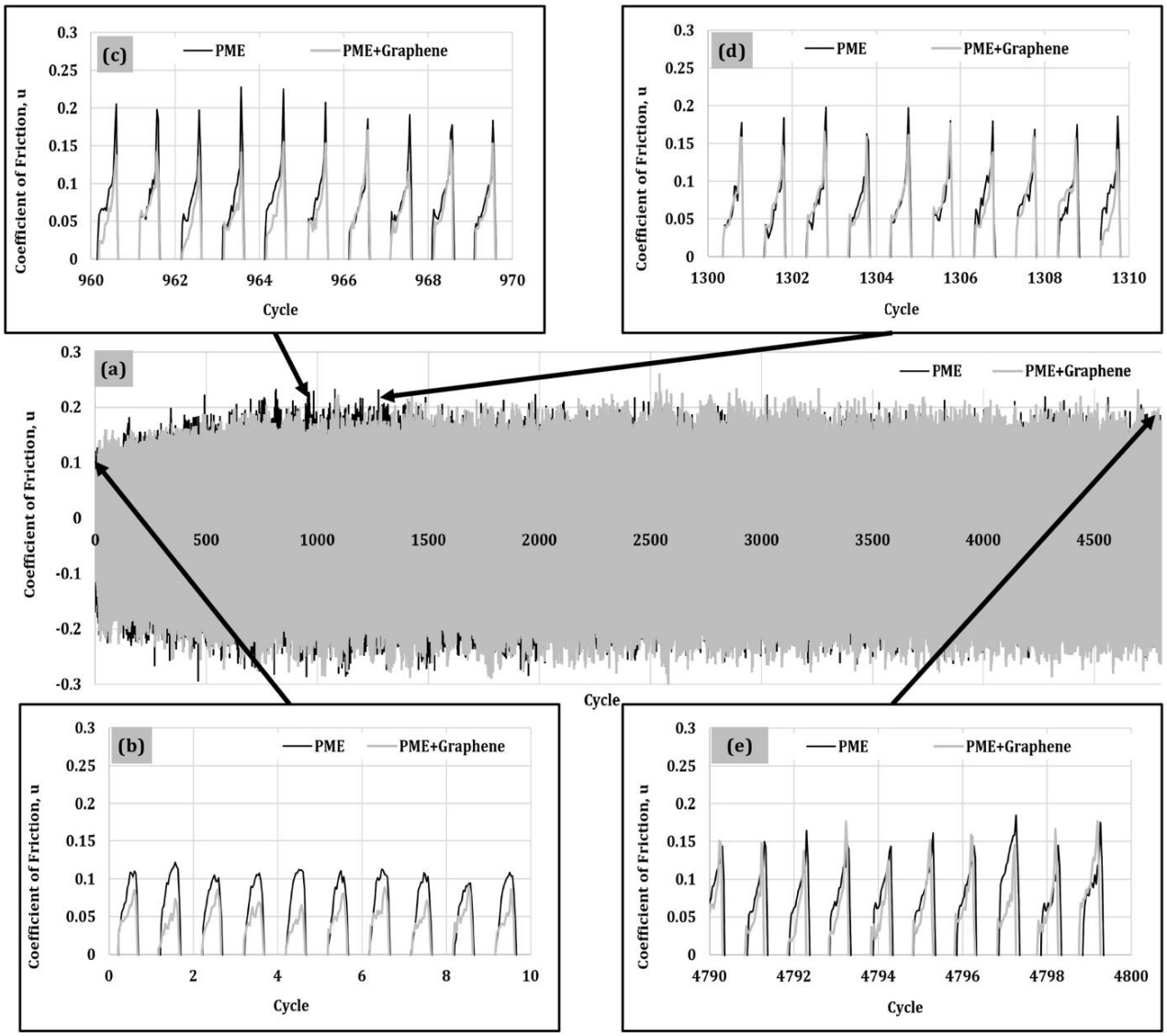


**Fig. 5.** Result of friction tests indicating friction coefficient of the entire 4800 sliding cycles (a), friction coefficient at the first 10 sliding cycle (b), sliding cycle 960 to 970 (c), sliding cycle 1300 to 1310 (d), and sliding cycle 4790 to 4800 (e).

However, it seems that this low friction condition in the case of S2 did not persist at the latter stage of sliding. As illustrated in Fig. 7(a)-(b), both the CoF graphs of sample S1 and S2 indicate a relatively similar values at sliding cycle no. 1300, i.e. sliding distance of 22.5 m. This result implies that the presence of graphene nanosheet in the palm methyl ester does not affect the CoF value of self-mated AISI52100 in the long run.

Despite the similar value of CoF for both sample S1 and S2 at the latter stage of sliding distance, it is obvious that the worn surface of the metal under S2 consisted of a more uniformly distributed tribo-layer (Fig. 8). In the case of S1, the tribo-layer is found on localized spot and less distributed (Fig. 8(a)-(b)). But in the case of S2, the tribo-layer is found scattered and distributed in a relatively wider area on the worn scar (Fig. 8(d)) compared to that in the case of S1. The tribo-layer in the case of S2 (Fig. 8(d)) also seems thinner than that in the case of S1 (Fig. 8(b)). The distribution of the tribo-layer on the contact interface can also be observed in Fig. 9(a) and Fig. 10(a) as the "blackish" layer of the worn area. It seems that such blackish layer is denser and covers a wider area in the case of S2 compared to that in S1.

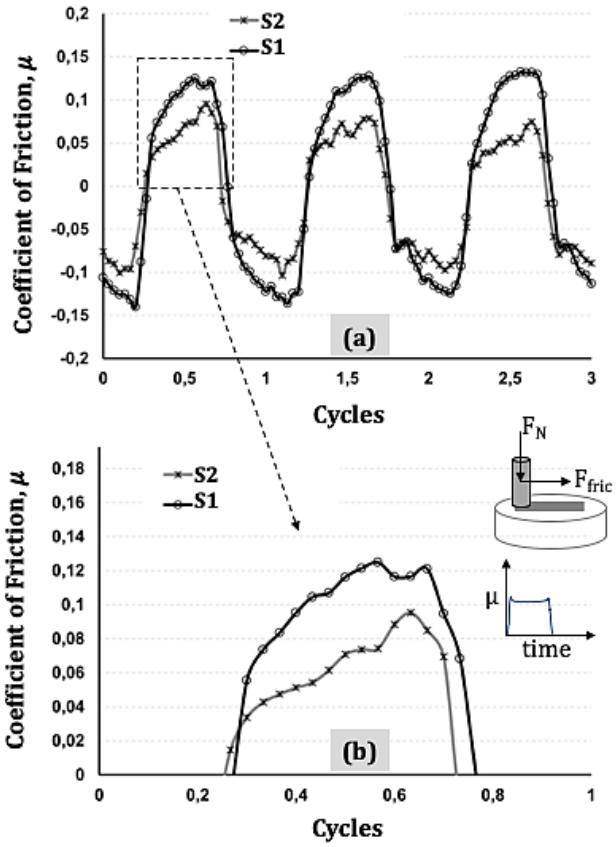


**Fig. 6.** At early sliding cycles, the friction coefficient decreases due to the presence of graphene nanosheets in the methyl ester. CoF at the first 3 sliding cycles (a), at the fist sliding half-cycle (b).

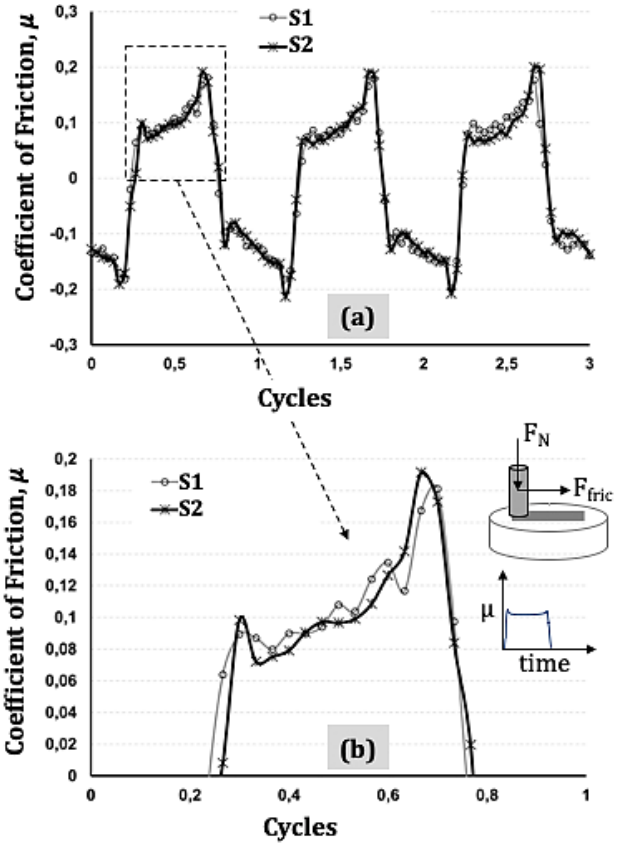


**Fig. 7.** At 22.5 m sliding distance (cycle no 1300 to 1303), the friction coefficient shows a similar value for both PME (S1) and PME+graphene (S2) condition. CoF at sliding cycles no. 1300 to 1303 (a), detail of CoF for sliding cycle no. 1300 (b).

Energy-dispersive X-ray Spectroscopy images indicate that the tribo-layer is dominated by Oxygen at both S1 and S2 condition, as observed in Fig. 9(d) and Fig. 10(d). However, the trace of Oxygen is found in a wider area in the case of S2 (Fig. 10(d)), which confirms the wider formation area of the tribo-layer in the case of S2.

Despite the presence of graphene in the lubricant, carbon element is hardly noticed on the contact interface. However, a closer look at Fig. 9(c) and Fig. 10(c) indicates a possibility of scattered carbon elements on the contact area where the tribo-layer located. The carbon traces seem also denser in the case of S2 (Fig. 10(c)) compared to that in the case of S1 (Fig. 9(c)); an indication of the presence of graphene particles in lubricant S2.

Based on the results, the wear mechanisms for the case of S1 (PME) can be proposed as tribo-layer formation by tribo-chemical oxidation process. The tribo-layer, which is oxygen rich, could be formed by the tribo-chemical process involving oxidation of metallic elements from the bulk material.

A tribo-chemical reaction between the lubricant additives and the surface of the friction pair can form a chemical reaction film [24]. It has been shown that a solid tribofilm can be produced by a base oil, particularly if it is catalically active [25]. In this study, the palm methyl ester has a significant amount of oxygen content and it could immediately react with the metallic material once it is released due to friction process, especially as high contact pressure. Here, carbon material seemed not involved in the process. The tribo-layer, developed on a concentrated location on the worn area, seems in ductile behaviour; a further indication of the absence of carbon in it. In the case of SUS304 material tribo-pair, the oxidation process involved the manganese material from the bulk that is more reactive than iron [9]. However, in this case, it seems that the oxidation layer is composed of Fe-O, as shown in Fig. 9(d).

On the other hand, for the case of S2 (PME+graphene nanosheets), the graphene particles could enter the surface in contact soon after the sliding starts. It seems they have acted as

the protective layer to reduce the shearing force among the asperities to reduce the friction. Graphene is two dimensional in structure and when used as additives in lubricant, it can easily enter the surface in contact, be adsorbed on asperities, and form the tribo-layer or transfer film [26]. As a result, low friction was achieved from the beginning of sliding (Fig. 6(b)). During the relative motion of friction, the graphene particles are subjected to both normal and shear forces. Due to the two dimensional and extremely thin laminated structure, the layers can effectively engage in the lubrication process to form the tribo-layer thus protecting the material from excessive wear [27,28]. Such mechanism seems occurred in this case of PME+graphene test condition.

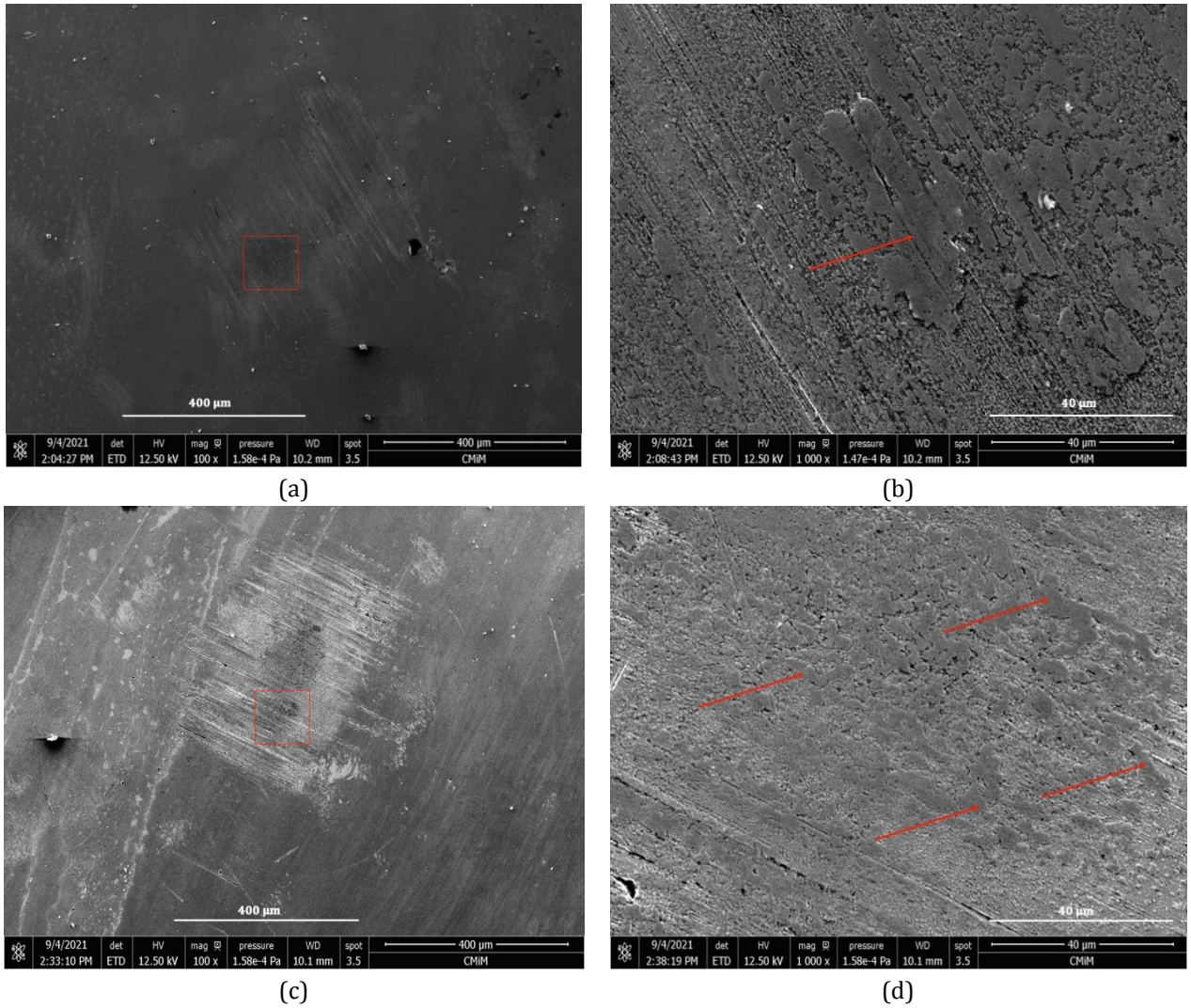


**Fig. 8.** Wear scar on the pin under S1 (a)-(b) and under S2 (b)-(c) with arrows pointing tribo-layer.

However, as the sliding progressed, tribo-oxidation occurred. But here in this case, the tribo-layer formed on the contact interface could mix with the graphene particles, resulting in a less ductile film. Therefore, the tribo-layer was formed in a smaller size and spread in a relatively wider contact area, as indicated in Fig. 8(d) and Fig. 10(a). The lumped form of graphene sheets, as shown in Fig. 2, could also be broken to smaller pieces of particles as friction continues, and involved in the tribo-oxidation process at a local spot. Therefore, the tribo-layer in this case could constitute carbon, oxygen, and metallic material from the bulk. As it can be observed from Fig. 10(c), the carbon elements on the contact interface is more observable that that in Fig. 9(c).

Other possibility is that smaller graphene particles adsorb to the micropores on the contact interface to form the protective film. Smaller sheet diameter also has more degree of defect and easily transferred by the lubricant to a region not covered by graphene [29].

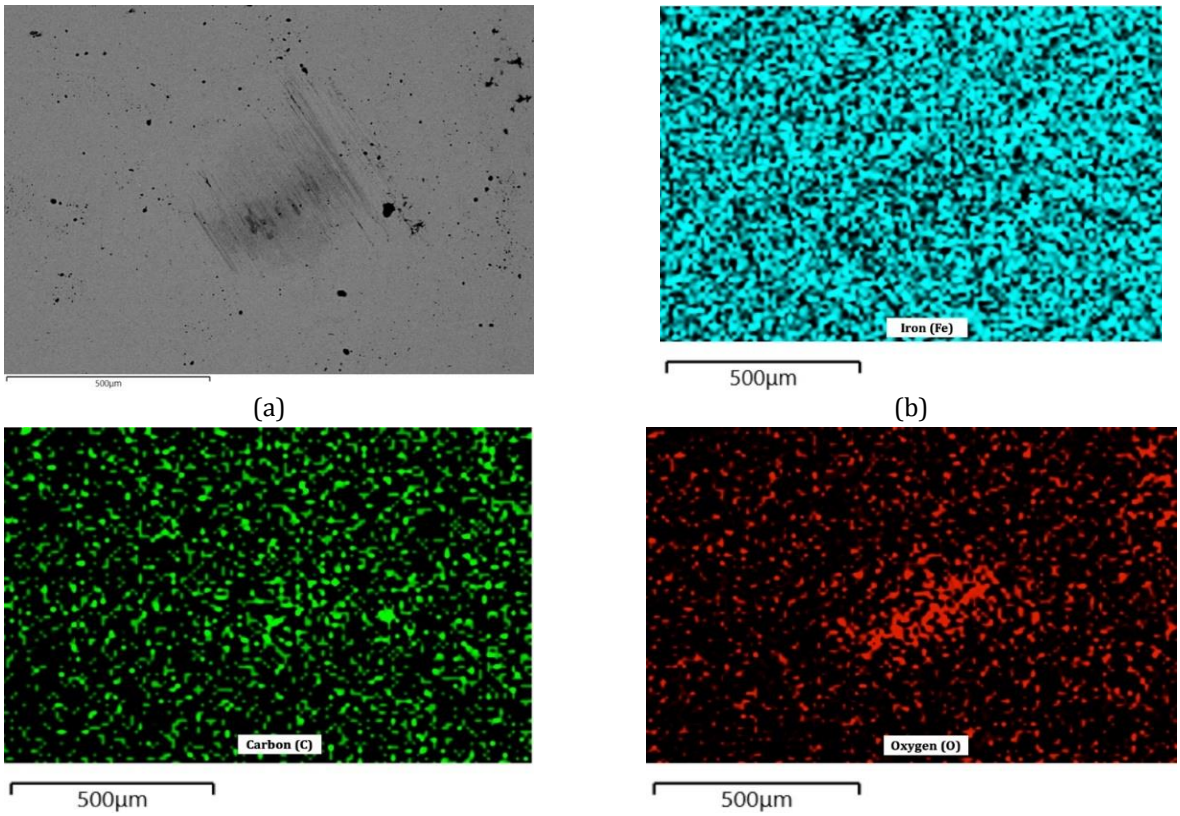


**Fig. 9.** EDX map of the wear scar on the pin under S1 (a). The map shows elements of Fe (a), C (b) and O (d). The map indicates the presence of oxygen-rich tribofilm on the contact interface (b).

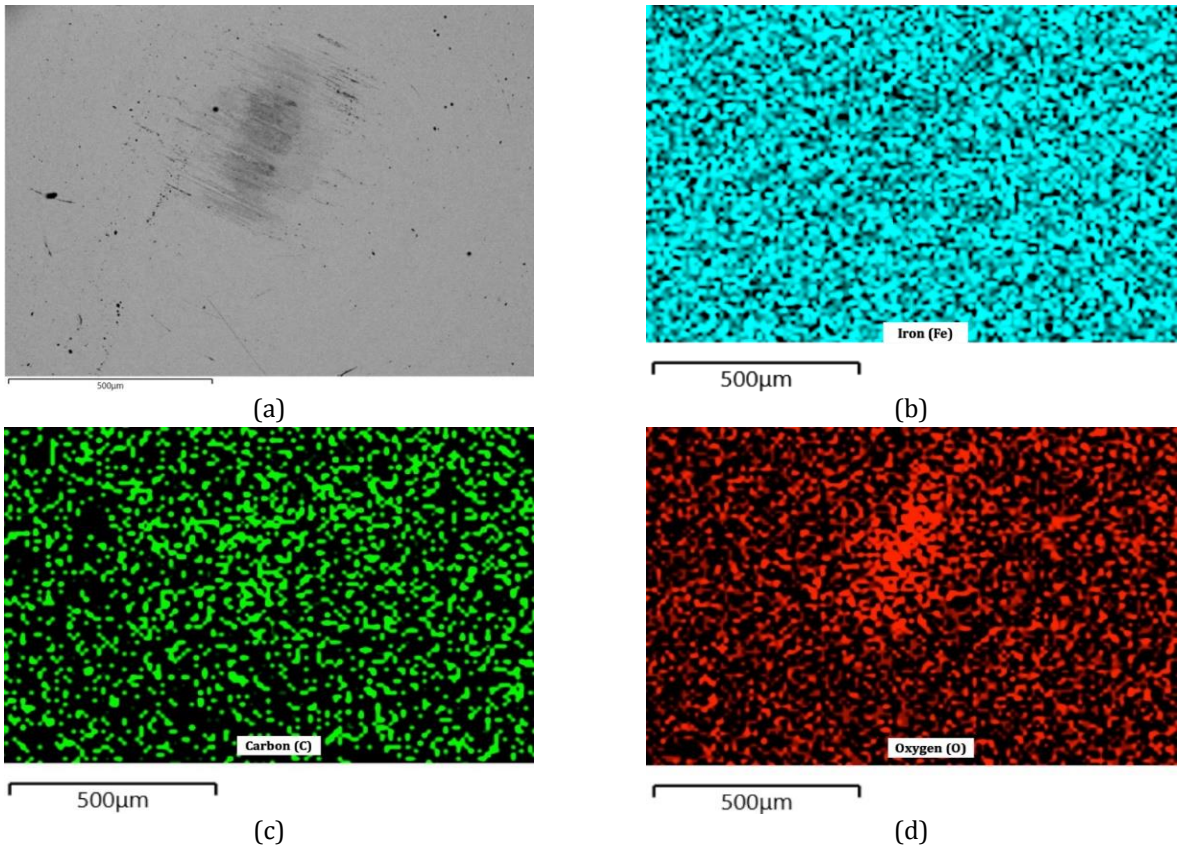


**Fig. 10.** EDX map of the wear scar on the pin under S2. The map shows elements of Fe (a), C (b) and O (d). The map shows the presence of oxygen-rich tribofilm on the contact interface.

In both S1 and S2 condition, the friction tests show a relatively similar value of coefficient of friction for the half end of the sliding distance. This implies that palm methyl ester alone has the ability to protect the contact interface from severe friction and wear. PME, without additional additives, has an ability to stimulate a frictional chemical reaction to form a chemical reaction film that prevent direct contact between sliding surfaces, preventing excessive friction and wear. Nevertheless, the presence of graphene particle as additive can further improve the tribological performance by enhancing the formation of protective film more uniformly across at contact interface.

## 4. CONCLUSION

An investigation on the tribo-layer characteristic formed on the contact interface of self-mated AISI52100 bearing steel lubricated by palm methyl ester containing graphene nanosheet has be conducted. The characteristics were compared to those lubricated by palm methyl ester without the nanoparticles. The results can be summarized as follows:

1. The friction and wear characteristics of AISI52100 bearing steel were not much different with or without the presence of graphene nanosheet in the palm methyl ester. A relatively similar values of friction coefficient were achieved for both conditions after sliding distance of 72 m at 1.2 GPa initial contact pressure. The effect of graphene to friction was effective only at the beginning of sliding, presumably due to the ability of graphene nanosheet entering the contact interface immediately after the friction started.
2. Tribo-chemical oxidation seems occurred during the friction at both conditions. In both cases, the tribo-layer comprises of oxygen and metallic material, presumably Fe-O. However, with the presence of graphene nanosheet in the lubricant, the tribo-layer was formed scattered on a wider contact area with more observable carbon element. It seems that the graphene nanosheet broke into smaller pieces and incorporate into the local spot tribo-layer.
3. The results imply that palm methyl ester can be used effectively as a lubricant, with or without graphene particles as additives, because it possesses an ability to form a protective film on the contact interface by tribo-chemical reaction.

**Acknowledgement**

Funding for this research is provided by Direktorat Riset dan Pengabdian Masyarakat, Kementrian Pendidikan, Kebudayaan, Riset, dan Teknologi Republik Indonesia with Penelitian Dasar Research Scheme Reference Number: 19/UN11.2.1/PT.01.03/DRPM/2022, which is highly acknowledged.

## REFERENCES

[1] P. Nowak, K. Kucharska, M. Kamiński, *Ecological and health effects of lubricant oils emitted into the environment*, International Journal of Environmental Research and Public Health, vol. 16, iss. 16. pp. 1-13, 2019, doi: 10.3390/ijerph16163002

[2] S. Soni, M. Agarwal, *Lubricants from renewable energy sources – a review*, Green Chemistry Letters and Reviews, vol. 7, iss. 4. pp. 359-382, 2014, doi: 10.1080/17518253.2014.959565

[3] F.J. Owuna, M.U. Dabai, M.A. Sokoto, S.M. Dangoggo, B.U. Bagudo, U.A. Birnin-Yauri, L.G. Hassan, I. Sada, A.L. Abubbakar, M.S. Jibrin, *Chemical modification of vegetable oils for the production of biolubricants using trimethylolpropane: A review*, Egyptian Journal of Petroleum, vol. 29, iss. 1, pp. 75-82, 2020, doi: 10.1016/j.ejpe.2019.11.004

[4] O. Farobie, E. Hartulistiyoso, *Palm Oil Biodiesel as a Renewable Energy Resource in Indonesia: Current Status and Challenges*, Bioenergy Research, vol. 15, pp. 93-111, 2022, doi: 10.1007/s12155-021-10344-7

[5] M. Gregory, Palm Oil Production, Consumption and Trade Patterns, available at https://www.fern.org/fileadmin/uploads/fern/Documents/2022/Palm_oil_production_comsumption_and_trade_pattern.pdf, accessed:20.03.2023

[6] M.A. Fazal, A.S.M.A. Haseeb, H.H. Masjuki, *Investigation of friction and wear characteristics of palm biodiesel*, Energy Conversion Management, vol. 67, pp. 251–256, 2013, doi: 10.1016/j.enconman.2012.12.002

[7] H.H. Masjuki, M.A. Maleque, *The effect of palm oil diesel fuel contaminated lubricant on sliding wear of cast irons against mild steel*, Wear, vol. 198, iss. 1–2, pp. 293–299, 1996, doi: 10.1016/0043-1648(96)07208-0

[8] Z. Fuadi, K. Adachi, *Properties of tribofilm formed on self-mated stainless steel lubricated by palm methyl ester mixed petroleum diesel fuel*, Lubrication Science, vol. 33, iss. 6, pp. 345-357, 2021, doi: 10.1002/ls.1557

[9] Z. Fuadi, K. Adachi, T. Muhammad, *Formation of Carbon-Based Tribofilm Under Palm Methyl Ester*, Tribology Letters, vol. 66, iss. 88, pp. 1-10, 2018, doi: 10.1007/s11249-018-1036-8

[10] J. Zhao, Y. Huang, Y. He, Y. Shi, *Nanolubricant additives: A review*, Friction, vol. 9, iss. 5. 2021, doi: 10.1007/s40544-020-0450-8

[11] R. Li, X. Yang, D. Hou, Y. Wang, J. Zhang, *Superlubricity of carbon nanostructural films enhanced by graphene nanoscrolls*, Material Letters., vol. 271, 2020, doi: 10.1016/j.matlet.2020.127748

[12] V. Eswaraiah, V. Sankaranarayanan, S. Ramaprabhu, *Graphene-based engine oil nanofluids for tribological applications*, ACS Applied Materials and Interfaces, vol. 3, no. 11, pp. 4221-4227, 2011, doi: 10.1021/am200851z

[13] N.W. Awang, D. Ramasamy, K. Kadirgama, M. Samykano, G. Najafi, N.A.C. Sidik, *An experimental study on characterization and properties of nano lubricant containing Cellulose Nanocrystal (CNC)*, International Journal of Heat and Mass Transfer, vol. 130, pp. 1163-1169, 2019, doi: 10.1016/j.ijheatmasstransfer.2018.11.041

[14] J. Zhao, Y. Li, J. Mao, Y. He, J. Luo, *Synthesis of thermally reduced graphite oxide in sulfuric acid and its application as an efficient lubrication additive*, Tribology International, vol. 116, pp. 303-309, 2017, doi: 10.1016/j.triboint.2017.06.023

[15] S.T. Pham, K.A. Tieu, M. Ma, H. Zhu, H.H. Nguyen, D.R.G. Mitchell, M.J. Nancarrow, *Unusual Competitive and Synergistic Effects of Graphite Nanoplates in Engine Oil on the Tribofilm Formation*, Advanced Materials Interfaces, vol. 6, no. 19:1901081, 2019, doi: 10.1002/admi.201901081

[16] J. Zhao, Y. Li, Y. He, J. Luo, *In Situ Green Synthesis of the New Sandwichlike Nanostructure of Mn3O4/Graphene as Lubricant Additives*, ACS Applied Materials and Interfaces, vol. 11, no. 40, pp. 36931–36938, 2019, doi: 10.1021/acsami.9b08993

[17] M.F. Bin Abdollah, H. Amiruddin, A.D. Jamallulil, *Experimental analysis of tribological performance of palm oil blended with hexagonal boron nitride nanoparticles as an environment-friendly lubricant*, The International Journal of Advanced Manufacturing Technology, vol. 106, iss. 9–10, pp. 4183–4191, 2020, doi: 10.1007/s00170-019-04906-5

[18] M. Gulzar, H.H. Masjuki, M. Varman, M.A. Kalam, R.A. Mufti, N.W.M. Zulkifli, R. Yunus, R. Zahid, *Improving the AW/EP ability of chemically modified palm oil by adding CuO and MoS2 nanoparticles*, Tribology International, vol. 88, pp. 271-279, 2015, doi: 10.1016/j.triboint.2015.03.035

[19] Q. Wu, X. Xie, Y. Wang, T. Roskilly, *Experimental investigations on diesel engine performance and emissions using biodiesel adding with carbon coated aluminum nanoparticles*, Energy Procedia, vol. 142, pp. 3603-3608, 2017, doi: 10.1016/j.egypro.2017.12.251

[20] N. Murugan, H. Venu, J. Jayaraman, P. Appavu, *Emission and performance characteristics study on nanographene oxide additives doped palm oil methyl ester blend in a diesel engine*, International Journal of Ambient Energy, vol. 43, iss. 1, pp. 1304-1310, 2022, doi: 10.1080/01430750.2019.1697361

[21] C.M.K. Periyasamy, C. Manickam, *Experimental studies on stability of multi walled carbon nanotube with different oil based nanofluids*, Thermal Science, vol. 24, iss. 1, pp. 533-539, doi: 10.2298/TSCI190412432P

[22] D. Rahmadiawan, H. Abral, N. Nasruddin, Z. Fuadi, *Stability, Viscosity, and Tribology Properties of Polyol Ester Oil-Based Biolubricant Filled with TEMPO-Oxidized Bacterial Cellulose Nanofiber*, International Journal of Polymer Science, vol. 2021, 2021, doi: 10.1155/2021/5536047

[23] A.K. Rasheed, M. Khalid, W. Rashmi, T.C.S.M. Gupta, A. Chan, *Graphene based nanofluids and nanolubricants - Review of recent developments*, Renewable and Sustainable Energy Reviews, vol. 63, pp. 346-362, 2016, doi: 10.1016/j.rser.2016.04.072

[24] M. Ratoi, V.B. Niste, J. Walker, J. Zekonyte, *Mechanism of action of WS2 lubricant nanoadditives in high-pressure contacts*, Tribology Letters, vol. 52, iss. 1, pp. 81-91, 2013, doi: 10.1007/s11249-013-0195-x

[25] A. Erdemir, G. Ramirez, O.L. Eryilmaz, B. Narayanan, Y. Liao, G. Kamath, S.K.R.S. Sankaranarayanan, *Carbon-based tribofilms from lubricating oils*, Nature, vol. 536, pp. 67-71, 2016, doi: 10.1038/nature18948

[26] J. Sun, S. Du, *Application of graphene derivatives and their nanocomposites in tribology and lubrication: A review*, RSC Advances, vol. 9, pp. 40642-40661, 2019, doi: 10.1039/c9ra05679c

[27] Y. Xu, Y. Peng, K.D. Dearn, X. Zheng, L. Yao, X. Hu, *Synergistic lubricating behaviors of graphene and MoS2 dispersed in esterified bio-oil for steel/steel contact*, Wear, vol. 342–343, pp. 297-309, 2015, doi: 10.1016/j.wear.2015.09.011

[28] J. Lin, L. Wang, G. Chen, *Modification of graphene platelets and their tribological properties as a lubricant additive*, Tribology Letters, vol. 41, pp. 209-215, 2011, doi: 10.1007/s11249-010-9702-5

[29] R. Rosentsveig, A. Margolin, A. Gorodnev, R. Popovitz-Biro, Y. Feldman, L. Rapoport, Y. Novema, G. Naveha, R. Tenne, *Synthesis of fullerene-like MoS2 nanoparticles and their tribological behavior*, Journal of Materials Chemistry, vol. 19, pp. 4368-4374, doi: 10.1039/b820927h